PERFORATED CLOSED-CELL METAL FOAM FOR ACOUSTIC APPLICATIONS

Kamil C. Opiela[1]   **Tomasz G. Zieliński**[1]   **Tomáš Dvorák**[2]   **Stanislav Kúdela Jr.**[2]

[1] Institute of Fundamental Technological Research, Polish Academy of Sciences,
ul. Pawińskiego 5B, 02-106 Warsaw, Poland

[2] Institute of Materials and Machine Mechanics, Slovak Academy of Sciences,
Dúbravská cesta 9, 845 13 Bratislava, Slovakia

`kopiela@ippt.pan.pl`   `tzielins@ippt.pan.pl`   `ummsdvor@savba.sk`   `ummskudm@savba.sk`

ABSTRACT

Despite very good mechanical and physical properties such as lightness, rigidity and high thermal conductivity, closed-porosity metal foams alone are usually poor acoustic treatments. However, relatively low production cost weighs them in many applications in favour of their open-cell equivalents. In the present paper, this attractive and popular material is subject to consideration from the point of view of the improvement of its sound absorption characteristics. A classic method of perforation is proposed to open the porous interior of the medium to the penetration of acoustic waves and therefore enhance the dissipation of their energy. The interaction between the perforation diameter and closed-cell microstructure as well as its impact on the overall sound absorption of a similar foam were already studied in 2010 by Chevillotte, Perrot and Panneton, so these topics are not discussed much in this work. On the other hand, the objective here is to investigate if one can efficiently approximate the wave propagation phenomenon in real perforated heterogeneous materials with closed porosity of irregular shape by means of their simplified three-dimensional representation at the micro-level. The applied multi-scale modelling of sound absorption was confronted with measurements performed in an impedance tube. Moreover, as expected, numerical and experimental comparisons with relevant perforated solid samples show great benefit coming from the presence of a porous structure in the foam, although it was initially closed.

1. INTRODUCTION

The propagation and suppression of acoustic (i.e. pressure) waves in open-cell foams have been research topics of many scientists until today. Various materials have been investigated: open-cell aluminium foams [1, 2], ceramic foams with spherical pores [3], polyurethane foams with thin membranes [4], polymeric [5–9], double-porosity [10], and additively manufactured [11] foams, adaptable materials [12, 13], micro-perforated plates with complex patterns of micro-slits [14, 15], and even meta-porous [16,17] as well as active [18] configurations. Therefore, such media are quite well documented in the literature in terms of attenuating the energy of acoustic waves.

Sound absorption by virtually closed-cell rigid foams is much less studied. First achievements in this field for rolled (compressed) and heat-treated closed-porosity metal foams are well summarised in [19, Chap. 12] and [20, 21], respectively. However, there is rather a limited number of contributions that deal with the utilisation of perforated closed-porosity materials in acoustics. Chevillotte, Perrot and Panneton [22] are among the few authors who have investigated the link between the noise attenuation performance and the microgeometry of a drilled cellular medium with closed regular pores. In this paper and its extended version [23], on the other hand, one finds the modelling results confirmed by experimental data and obtained for:

(a) a *heterogeneous* (with eminently irregular pore sizes and shapes) as well as *three-dimensional* (3D) real foam microstructure;

(b) a representative real (non-periodic) geometry reconstructed from *computer tomography scans*; and

(c) an idealised (approximative) *periodic unit cell* that successfully characterises complicated material morphology.

2. CLOSED-POROSITY ALUMINIUM FOAM

A panel of an aluminium foam with (nearly) closed porosity, known as the Alulight, was prepared at the Institute of Materials and Machine Mechanics in Bratislava, Slovakia. It was manufactured under pressure in powder metallurgy technology, with an alloy comprising 10 wt.% of Si and Al balanced (i.e. AlSi10) as the foamable precursor, and 0.8 wt.% of TiH_2 as the blowing agent. This method is very well established and has already led to many publications, e.g. [24–32].

The cylindrical specimen of a diameter about 29 mm and thickness (height) 50 mm was cut out from the material panel using an electric discharge machine (Fig. 1a). The application of such processing, in turn, guaranteed that it does not contain dense surface skin and is accurate. The resulting structure of the sample was verified under a digital microscope and by the help of computer tomography (CT) scans made on the GE Nanotom 180 device with the voxel size 0.03 mm. Fig. 1b is the picture of the top surface of
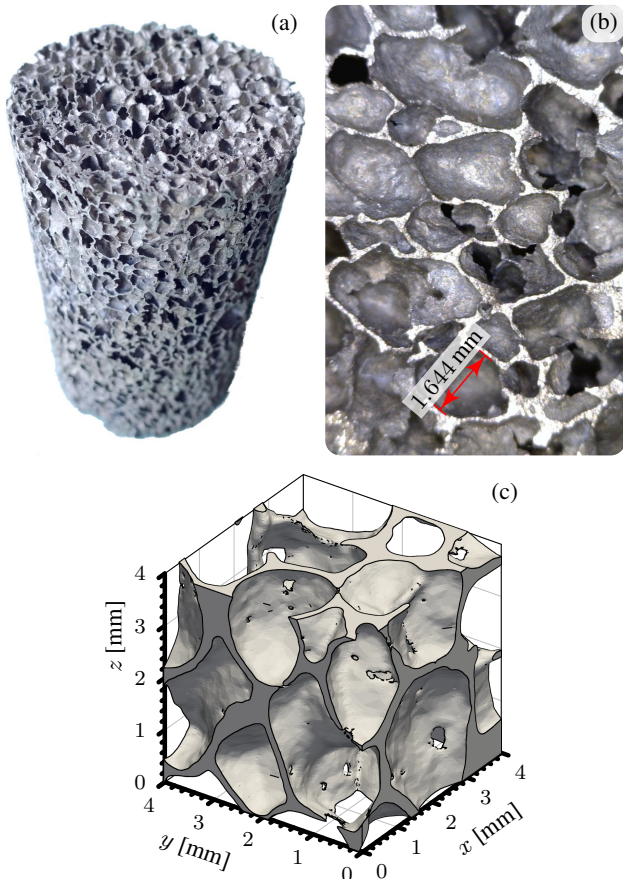
Figure 1: The sample of aluminium foam under investigation: (a) general view (the top and lateral sides are visible); (b) enlarged view on the top of the sample (at height $z = 50\,\text{mm}$); and (c) typical skeleton microgeometry.

the specimen seen at certain magnification. It indicates that most of the pores have somewhat oblate shape and are connected to the adjacent air voids by either very tiny channels or narrow cracks on their walls (see also Fig. 1c). In effect, at some distance from the incident surface the fluid domain becomes dead-ended which strongly restricts acoustic wave penetration through the medium to a short region. The material can therefore be considered as having effectively closed cellular microgeometry from the perspective of sound propagation and absorption.

The computer analysis of microscopic and CT images corresponding to particular sample cross-sections revealed that pores are mostly elongated in the axial direction or parallel to the xy base, with an average size of $1.7\,\text{mm}$ (cf. [31]). It was observed that there are places in the sample where some pores substantially distinguish in size from others in the vicinity, which is inherently caused by the chaotic nature of the foaming process. However, the material can be treated as isotropic due to high total porosity—0.8 calculated from the CT scan, and 0.83 determined based on a precise measurement of sample weight, assuming perfect geometry and the density of the metal alloy equal to $2650\,\text{kg/m}^3$—as the degree of anisotropy of a foam usually decreases with increasing porosity [25, 31, 32].

3. SAMPLES FOR ACOUSTIC TESTING

Two metal foamed and one polymer solid samples were prepared, each of them in the form of a cylinder with a diameter close to $29\,\text{mm}$ and thickness (height) $50\,\text{mm}$. The first aluminium specimen had original porous microstructure. The two remaining samples were obtained by perforating the first sample and a solid cylinder using a 2-mm bit to reflect the regular pattern of parallel holes spaced every $4\,\text{mm}$, shown in Fig. 2. Such modification in the case of the solid sample yielded the actual porosity of approximately 0.2. Due to opening of initially closed pores in the original specimen while the drilling process, the open porosity of the corresponding perforated foam sample was appropriately higher. Nevertheless, its specific value is unknown.
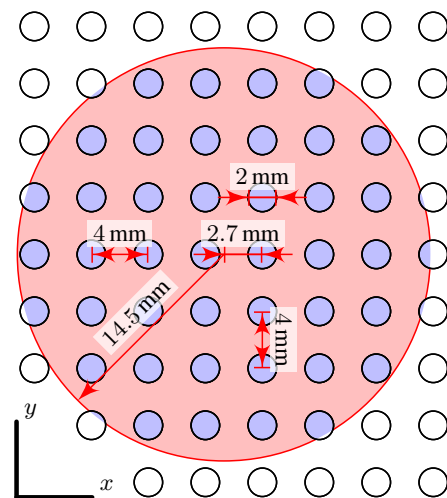

Figure 2: Dimensions of the applied perforation pattern. Red colour represents a sample, whereas the removed material is marked in blue.

Figs 1a and 3 present the tested samples. While spark erosion was used to cut out the original foam sample from the material panel, as already remarked in Sec. 2, the polymer sample was fabricated in the Fused Deposition Modelling additive manufacturing technology [33]. The top, bottom and lateral surfaces of the latter were then machined on a lathe to precisely meet the desired dimensions. The perforation holes were either drilled on a milling machine controlled numerically in the case of the metal foam, or were broached in the polymer sample with an electric drill guided by 3D printed channels of a smaller diameter. Perfect circular shapes of the specimens and good consistency of their characteristic sizes with the designed values were confirmed by measuring their key dimensions and carefully inspecting their quality under a microscope.

4. ACOUSTIC MEASUREMENTS AND MODELLING OF THE ALUMINIUM FOAM

4.1 Experimental configuration

Acoustic measurements were done in a Brüel & Kjær impedance tube of a diameter $29\,\text{mm}$ for frequencies be-
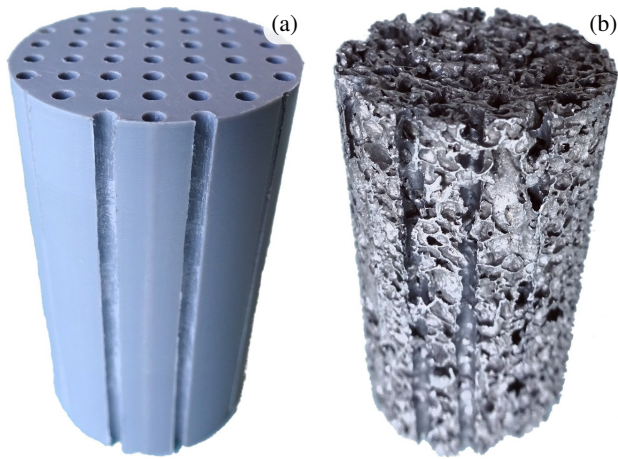
Figure 3: The manufactured perforated samples (the top and lateral sides are visible): (a) the perforated solid one; and (b) the perforated aluminium foam.

tween $0\,\mathrm{Hz}$ and $5200\,\mathrm{Hz}$. In fact, only the results above $500\,\mathrm{Hz}$ are valid for this tube size. Both configurations with and without an air gap of thickness $10\,\mathrm{mm}$ left between the sample and the terminating rigid piston were considered.[1] To eliminate the risk of impedance tube scuffing, the metal specimens were additionally wrapped with a $0.15\,\mathrm{mm}$-thick tape. The experiments were conducted according to the Two-Microphone Transfer Function Method [34] on well-fitted samples. This technique relies on reading the acoustic pressure at two predefined positions inside the tube. Based on the pressure levels and taking into account physical properties of air and geometrical dimensions of the tube, one evaluates the value of various acoustic indicators, including the normal incidence sound absorption coefficient, i.e. a frequency-dependent real quantity ranging from 0 (no attenuation) to 1 (perfect absorption).

4.2 Mathematical models

The equivalent-fluid approach for rigid-frame porous media [35] was utilised to confront the experimental sound absorption curves with analytical and numerical predictions. In this method the investigated open-porosity material is treated as a homogeneous fluid possessing its macroscopic acoustic properties expressed in the equivalent density and equivalent bulk modulus functions of frequency. These complex quantities are derived from the dynamic visco-inertial and dynamic thermal tortuosities, respectively, also varying with frequency, and from some real-valued parameters of the fluid saturating the pores. Provided that plane waves penetrate an equivalent fluid at normal incidence, which is assumed to be true within an impedance tube, the acoustic wave propagation in such a dispersive medium on the macroscale is governed by the Helmholtz equation of time-harmonic linear acoustics. Consequently, the surface acoustic impedance depends on the equivalent characteristic impedance and the

---

[1] Note that in the latter case the porous material-air system has the total thickness of 60 mm.

effective speed of sound in addition to other real parameters [36]. Then, the acoustic absorption coefficient is expressed through the surface acoustic impedance as well as the characteristic impedance of the pore-fluid [35].

The *analytical* approximations of the dynamic tortuosity functions for the considered perforated solid sample were computed from formulae incorporating the Bessel functions of the first kind of zero and first order [37].

On the other hand, the *numerical* dynamic tortuosities, which served to achieve all the numerical solutions from Sec. 5, are estimated by means of a hybrid multi-scale approach with the Johnson-Champoux-Allard-Pride-Lafarge (JCAPL) equivalent-fluid model for rigid-frame porous materials [35, 38–43]. It is based on eight fully geometric 'transport' parameters: the open porosity, (static) viscous permeability, (static) thermal permeability, (inertial) tortuosity, static viscous tortuosity, static thermal tortuosity, viscous characteristic length, and thermal characteristic length. Their values can be evaluated on a unit cell that sufficiently represents the fluid domain inside the porous microstructure of a given material. Except for the open porosity and thermal characteristic length, it is essentially required here to solve certain steady-state boundary value problems (for the corresponding formulae see, e.g. [2, 15, 22, 44–47]). All in all, the JCAPL model relationships allow to calculate the dynamic tortuosities and, finally, the sound absorption coefficient.

5. RESULTS

The finite element method [48, 49] was used to perform the numerical analyses and figure out the transport parameters for acoustic waves propagating along the thickness of the specimens. For the case of the perforated solid sample, the whole problem is reduced to two spatial dimensions due to the presence of infinitely many symmetry planes of the perforation pattern in the axial direction [15]. The whole section-area of the fluid region was selected for the simulations instead of just a unit cell in order to better mirror the actual porosity of the manufactured specimen. The domain in question is indicated by blue colour in Fig. 2.

However, more complex geometries usually entail the necessity of finding symmetrical or periodic 3D numerical solutions within a unit cell for the purposes of the multi-scale JCAPL technique. Finite element computations were carried out for the scanned cubic ($4 \times 4 \times 4\,\mathrm{mm}$) fragment of the original porous microstructure shown in Fig. 1c. Its porosity equal to 0.797, and thermal characteristic length about $0.706\,\mathrm{mm}$, are very close to the reference values got from a set of CT images of a $12 \times 12 \times 24$-mm interior part of the primary foam sample—0.799 and $0.7557\,\mathrm{mm}$, respectively. This is one of the reasons why the chosen unit cell was assumed representative for the material. Then, the proposed perforation pattern (Fig. 2) was applied to the same skeleton element in the direction of acoustic wave propagation (viz. in the z-direction; see Fig. 4a) and the simulations were run on the corresponding air volume. In this situation, the porosity and thermal characteristic length increase to 0.835, and $0.891\,\mathrm{mm}$, respectively.
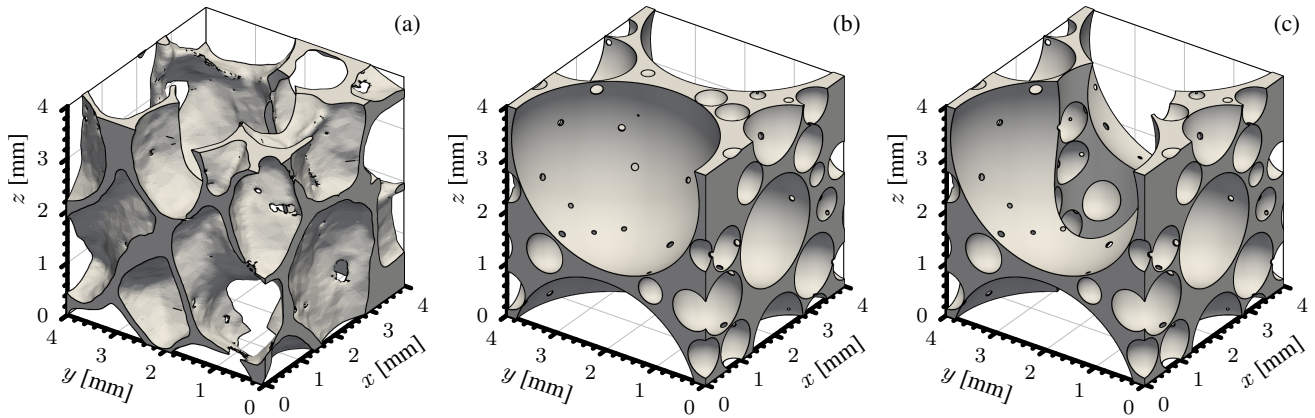
Figure 4: Unit cell skeletons: (a) representative for the primary microgeometry with the perforation pattern applied to it; and (b, c) approximating the internal structure of the original metal foam by means of a periodic porosity composed of spheres (b) without as well as (c) with the perforation channel.

A periodic 4-mm cubic cell approximating the morphology of the metal foam was created in the next step as the output of a random generation procedure (see Fig. 4b). Its microgeometry consists of 50 spherical pores with diameters varying between 0.22 mm and 3.8 mm (about 0.81 mm in average) and has the open porosity equal 0.74, while its thermal characteristic length is 0.65 mm. The mean pore size read from microscopic measurements (Fig. 1b) as well as the target porosity and thermal characteristic length values (i.e. 0.799 and 0.7557 mm, respectively) in particular were maintained as much as possible by accepting only befitting positions and radii of pores during the generation process. This was feasible because just the shape of a unit cell is needed to determine these two transport parameters. It was also ensured that the sequentially drawn spheres are not too far from the closest already found instance, are linked to it, and do not overlap with other pores. Similarly to the case of the cell coming from the CT scan, computations were made for the perforated variant of the approximative skeleton as well (Fig. 4c) with the porosity of over 0.8 and thermal characteristic length equal to 0.84 mm.

Figs 5 and 6 present the received experimental and modelling results. The impedance tube measurements were performed on the samples inserted in such a way that their top side was turned towards the loudspeaker generating white noise. The plots show that:

- the original, non-perforated foam sample *has* open pores (the values of the absorption coefficient are significantly higher than zero), but only within a restricted area beginning at the incident face—acoustic waves do not penetrate deeply inside it nor in all its volume, and, in particular, do not reach the air gap behind the specimen so that the presence of it has no effect on the absorption (see the black experimental curve pertinent to the lack of perforation left in each figure for reference). One may thus conclude that the overall 'effective' porosity in the sample is closed;

- the analytical and numerical results incorporating the JCAPL model included in Fig. 5 are in perfect agreement;

- the experimental sound absorption obtained on the solid (polymer) sample does correspond well to the relevant analytical and numerical estimations both for the configuration with and without the air gap behind the sample (Fig. 5). Theoretically very low absorption level in between peaks is satisfactorily reproduced, which is indicative of a good surface finish in the sample, and its dimensional consistency with the designed geometry;

- the perforated metal foam sample, on the other hand, do outperform its solid (i.e. polymer) equivalent in noise suppression (Fig. 5). It is generally much better in a wide spectrum of frequencies. Its first quarter wavelength layer resonance is shifted to lower frequencies (about 1.1 kHz) for the case of no air gap just thanks to the applied perforation. Moreover, the relevant absorption curve has more peaks in the considered frequency range than the one pertaining to the polymer sample when the gap is present;

- it is actually quite difficult to mimic the complex experimental behaviour of a real aluminium isotropic foam of this sort (see Fig. 6). Both attempts (approximation- and CT-based) gave correct predictions only for the perforated case, which for acoustic closed-porosity foams is of greater importance from the point of view of designing a perforation pattern that fulfils specific operational requirements. The sound absorption of the non-perforated material is clearly overestimated by the applied modelling, regardless of the gap configuration. This is probably because the utilised unit cells (and hence the simplified artificial materials composed entirely of them) have fully open porosity that enables complete penetration of acoustic waves within their air-filled pores without strong resistance due to narrow pore interconnections, in contrast to the real foam. However, the general character of the experimental curve is reflected to some degree, especially by using the approximate cell.
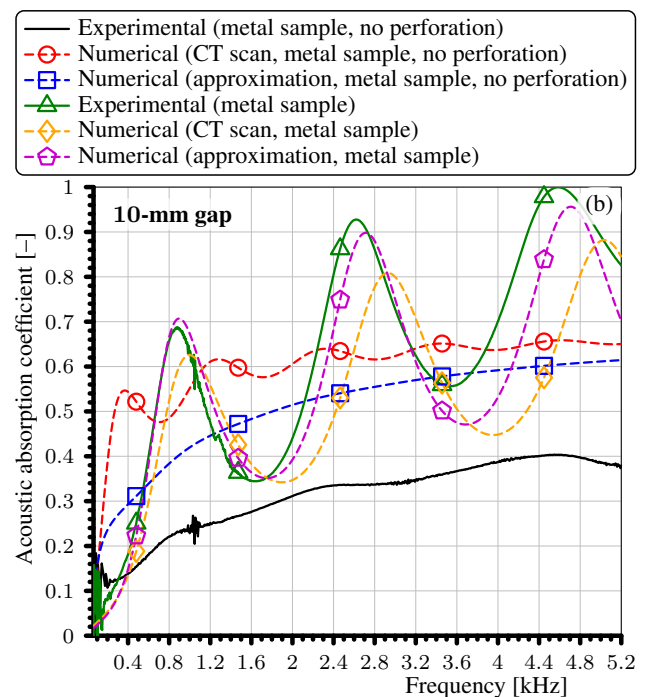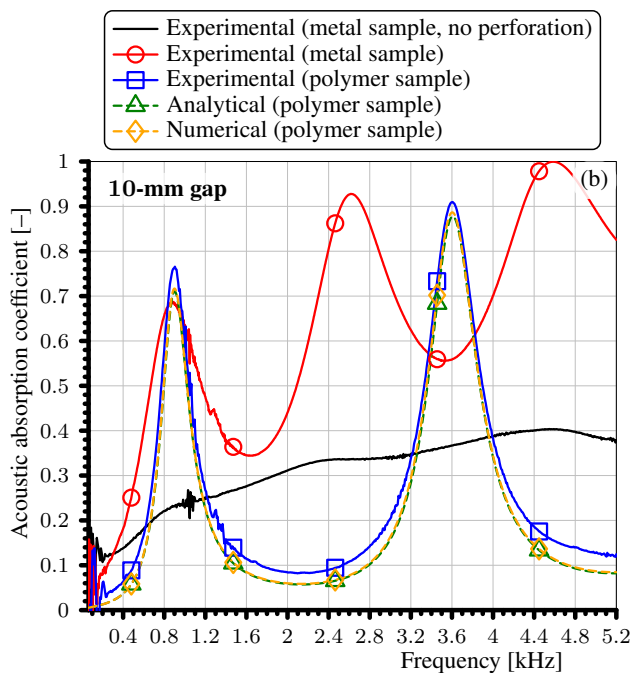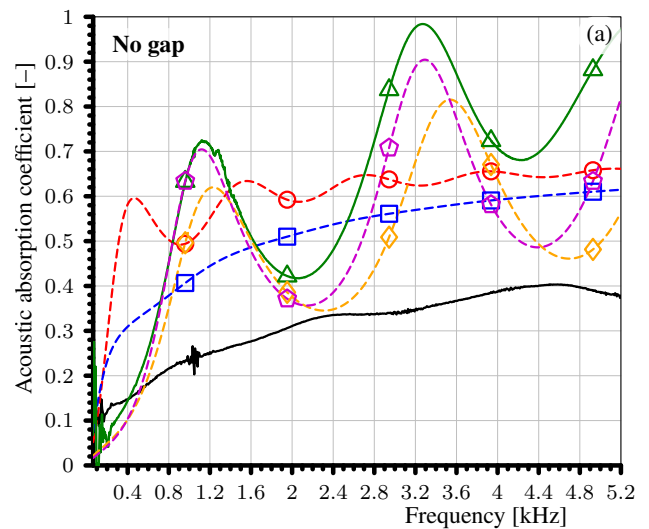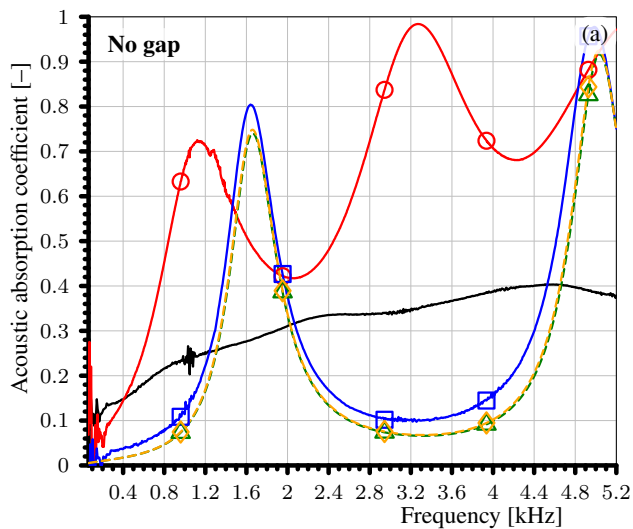
Figure 5: Normal incidence acoustic absorption coefficient for the samples: (a) without an air gap; (b) with a 10-mm air gap between the material and the rigid impedance tube termination.

Figure 6: Numerical predictions (confronted with experiments) of the normal incidence acoustic absorption coefficient based on the CT-scanned (non-periodic) and approximate (periodic) unit cells: (a) without an air gap; and (b) with a 10-mm air gap between the material and the rigid impedance tube termination.

6. CONCLUSIONS

It is usually profitable to drill through the aluminium foam and therefore open its porosity if one considers its acoustic application as a noise absorber. The studied perforated porous material is much better in sound absorption than its solid equivalent. In addition, it weighs less than a metal (or even polymer) perforated plate of the same thickness, and still can be successfully used in harsh conditions, e.g. on hot surfaces of an engine or turbine.

As a part of the present work, the real internal structure of the original foam was approximated by means of a random periodic arrangement of spherical pores. The final results suggest that the approach works fairly well for this sort of mass-produced porous materials. Nonethe-

less, there are many factors that influenced the accuracy of the predictions made, such as the origin of a representative unit cell isolated from the foam microgeometry, selection of the cell-centred position at which the perforation was applied, or the particular specification of the generation constraints imposed on the approximative unit cell (maximal pore diameter, maximal window diameter between two linked pores, target number of pores, etc.).

7. REFERENCES

[1] C. Perrot, R. Panneton, and X. Olny, "Periodic unit cell reconstruction of porous media: Application to open-cell aluminum foams," *J. Appl. Phys.*, vol. 101, pp. 1–11, article 113538, June 2007.

[2] C. Perrot, F. Chevillotte, and R. Panneton, "Dynamic viscous permeability of an open-cell aluminum foam: Computations versus experiments," *J. Appl. Phys.*, vol. 103, pp. 1–8, article 024909, Jan. 2008.

[3] T. G. Zieliński, "Generation of random microstructures and prediction of sound velocity and absorption for open foams with spherical pores," *J. Acoust. Soc. Am.*, vol. 137, pp. 1790–1801, Apr. 2015.

[4] K. Gao, J. A. W. van Dommelen, and M. G. D. Geers, "Microstructure characterization and homogenization of acoustic polyurethane foams: Measurements and simulations," *Int. J. Solids Struct.*, vol. 100–101, pp. 536–546, Dec. 2016.

[5] C. Perrot, F. Chevillotte, M. T. Hoang, G. Bonnet, F.-X. Bécot, L. Gautron, and A. Duval, "Microstructure, transport, and acoustic properties of open-cell foam samples: Experiments and three-dimensional numerical simulations," *J. Appl. Phys.*, vol. 111, pp. 1–16, article 014911, Jan. 2012.

[6] O. Doutres, M. Ouisse, N. Atalla, and M. Ichchou, "Impact of the irregular microgeometry of polyurethane foam on the macroscopic acoustic behavior predicted by a unit-cell model," *J. Acoust. Soc. Am.*, vol. 136, pp. 1666–1681, Oct. 2014.

[7] J. H. Park, K. S. Minn, H. R. Lee, S. H. Yang, C. B. Yu, S. Y. Pak, C. S. Oh, Y. S. Song, Y. J. Kang, and J. R. Youn, "Cell openness manipulation of low density polyurethane foam for efficient sound absorption," *J. Sound Vib.*, vol. 406, pp. 224–236, Oct. 2017.

[8] J. H. Park, S. H. Yang, H. R. Lee, C. B. Yu, S. Y. Pak, C. S. Oh, Y. J. Kang, and J. R. Youn, "Optimization of low frequency sound absorption by cell size control and multiscale poroacoustics modeling," *J. Sound Vib.*, vol. 397, pp. 17–30, June 2017.

[9] K. Gao, J. A. W. van Dommelen, and M. G. D. Geers, "Investigation of the effects of the microstructure on the sound absorption performance of polymer foams using a computational homogenization approach," *Eur. J. Mech. A-Solid.*, vol. 61, pp. 330–344, Jan.–Feb. 2017.

[10] F. Chevillotte, C. Perrot, and E. Guillon, "A direct link between microstructure and acoustical macro-behavior of real double porosity foams," *J. Acoust. Soc. Am.*, vol. 134, pp. 4681–4690, Dec. 2013.

[11] T. G. Zieliński, "Pore-size effects in sound absorbing foams with periodic microstructure: Modelling and experimental verification using 3D printed specimens," in *Proc. of ISMA2016 International Conference on Noise and Vibration Engineering/USD2016 International Conference on Uncertainty in Structural Dynamics* (P. Sas, D. Moens, and A. van de Walle, eds.), (Heverlee, Belgium), pp. 95–104, Katholieke Universiteit Leuven, Department of Mechanical Engineering, Sept. 2016.

[12] K. C. Opiela, M. Rak, and T. G. Zieliński, "A concept demonstrator of adaptive sound absorber/insulator involving microstructure-based modelling and 3D printing," in *Proc. of ISMA2018 International Conference on Noise and Vibration Engineering/USD2018 International Conference on Uncertainty in Structural Dynamics* (W. Desmet, B. Pluymers, D. Moens, and W. Rottiers, eds.), (Heverlee, Belgium), pp. 1091–1104, Katholieke Universiteit Leuven, Department of Mechanical Engineering, Sept. 2018.

[13] K. C. Opiela and T. G. Zieliński, "Microstructural design, manufacturing and dual-scale modelling of an adaptable porous composite sound absorber," *Compos. Part B-Eng.*, vol. 187, pp. 1–13, article 107833, Apr. 2020.

[14] K. Attenborough, "Macro- and micro-structure designs for porous sound absorbers," *Appl. Acoust.*, vol. 145, pp. 349–357, Feb. 2019.

[15] T. G. Zieliński, F. Chevillotte, and E. Deckers, "Sound absorption of plates with micro-slits backed with air cavities: Analytical estimations, numerical calculations and experimental validations," *Appl. Acoust.*, vol. 146, pp. 261–279, Mar. 2019.

[16] C. Lagarrigue, J.-P. Groby, O. Dazel, and V. Tournat, "Design of metaporous supercells by genetic algorithm for absorption optimization on a wide frequency band," *Appl. Acoust.*, vol. 102, pp. 49–54, Jan. 2016.

[17] J.-P. Groby, C. Lagarrigue, B. Brouard, O. Dazel, V. Tournat, and B. Nennig, "Using simple shape three-dimensional rigid inclusions to enhance porous layer absorption," *J. Acoust. Soc. Am.*, vol. 136, pp. 1139–1148, Sept. 2014.

[18] T. G. Zieliński, "Numerical investigation of active porous composites with enhanced acoustic absorption," *J. Sound Vib.*, vol. 330, pp. 5292–5308, Oct. 2011.

[19] M. F. Ashby, A. G. Evans, N. A. Fleck, L. J. Gibson, J. W. Hutchinson, and H. N. G. Wadley, eds., *Metal foams: A design guide*. Burlington: Butterworth-Heinemann, 1 ed., 2000.

[20] A. Byakova, S. Gnyloskurenko, Y. Bezimyanniy, and T. Nakamura, "Closed-cell aluminum foam of improved sound absorption ability: Manufacture and properties," *Metals*, vol. 4, pp. 445–454, Sept. 2014.

[21] A. Byakova, Y. Bezim'yanny, S. Gnyloskurenko, and T. Nakamura, "Fabrication method for closed-cell aluminium foam with improved sound absorption ability," *Procedia Mater. Sci.*, vol. 4, pp. 9–14, Aug. 2014. Proc. of the 8th International Conference on Porous Metals and Metallic Foams, Metfoam 2013.

[22] F. Chevillotte, C. Perrot, and R. Panneton, "Microstructure based model for sound absorption predictions of perforated closed-cell metallic foams," *J. Acoust. Soc. Am.*, vol. 128, pp. 1766–1776, Oct. 2010.

[23] K. C. Opiela, T. G. Zieliński, T. Dvorák, and S. Kúdela Jr., "Perforated closed-cell aluminium foam for acoustic absorption," *Appl. Acoust.*, article 107706, 2021. [in press].

[24] A. Adamčíková, B. Taraba, and J. Kováčik, "A study of porosity influence on thermal diffusivity of aluminium foam by experimental analysis and numerical simulation," in *Diffusion in Solids and Liquids V* (A. Öchsner, G. E. Murch, A. Shokuhfar, and J. M. P. Q. Delgado, eds.), vol. 297 of *Defect and Diffusion Forum*, pp. 814–819, Trans Tech Publications Ltd, Apr. 2010.

[25] J. Kováčik and F. Simančík, "Aluminium foam—Modulus of elasticity and electrical conductivity according to percolation theory," *Scripta Mater.*, vol. 39, pp. 239–246, June 1998.

[26] J. Kováčik, Ľ. Orovčík, and J. Jerz, "High-temperature compression of closed cell aluminium foams," *Kovové Mater.*, vol. 54, pp. 429–440, Jan. 2016.

[27] J. Kováčik, J. Jerz, N. Miníriková, L. Marsavina, and E. Linul, "Scaling of compression strength in disordered solids: Metallic foams," *Frattura Integr. Strutt.*, vol. 36, pp. 55–62, Mar. 2016.

[28] J. Kováčik, L. Marsavina, and E. Linul, "Poisson's ratio of closed-cell aluminium foams," *Materials*, vol. 11, pp. 1–11, article 1904, Oct. 2018.

[29] E. Linul, L. Marsavina, and J. Kováčik, "Collapse mechanisms of metal foam matrix composites under static and dynamic loading conditions," *Mat. Sci. Eng. A-Struct.*, vol. 690, pp. 214–224, Apr. 2017.

[30] Ľ. Orovčík, M. Nosko, J. Kováčik, T. Dvorák, M. Štěpánek, and F. Simančík, "Effects of chemical composition on the pore structure and heat treatment on the deformation of PM aluminium foams 6061 and 7075," *Kovové Mater.*, vol. 54, pp. 463–470, Jan. 2016.

[31] I. Sevostianov, J. Kováik, and F. Simaník, "Correlation between elastic and electric properties for metal foams: Theory and experiment," *Int. J. Fracture*, vol. 114, pp. 23–28, Apr. 2002.

[32] I. Sevostianov, J. Kováčik, and F. Simančík, "Elastic and electric properties of closed-cell aluminium foams: Cross-property connection," *Mat. Sci. Eng. A-Struct.*, vol. 420, pp. 87–99, Mar. 2006.

[33] T. D. Ngo, A. Kashani, G. Imbalzano, K. T. Q. Nguyen, and D. Hui, "Additive manufacturing (3D printing): A review of materials, methods, applications and challenges," *Compos. Part B-Eng.*, vol. 143, pp. 172–196, June 2018.

[34] ISO 10534-2, "Acoustics — Determination of sound absorption coefficient and impedance in impedance tubes — Part 2: Transfer-function method," ISO standard, International Organisation for Standardization, Case postale 56, CH-1211 Genève 20, Switzerland, Nov. 1998.

[35] J.-F. Allard and N. Atalla, *Propagation of sound in porous media: Modelling sound absorbing materials*. John Wiley & Sons, 2 ed., Oct. 2009.

[36] T. J. Cox and P. D'Antonio, *Acoustic absorbers and diffusers: Theory, design and application*. Taylor & Francis, 2004.

[37] K. Attenborough, "Microstructures for lowering the quarter wavelength resonance frequency of a hard-backed rigid-porous layer," *Appl. Acoust.*, vol. 130, pp. 188–194, Jan. 2018.

[38] D. L. Johnson, J. Koplik, and R. Dashen, "Theory of dynamic permeability and tortuosity in fluid-saturated porous media," *J. Fluid Mech.*, vol. 176, pp. 379–402, Mar. 1987.

[39] Y. Champoux and J.-F. Allard, "Dynamic tortuosity and bulk modulus in air-saturated porous media," *J. Appl. Phys.*, vol. 70, pp. 1975–1979, Aug. 1991.

[40] S. R. Pride, A. F. Gangi, and F. D. Morgan, "Deriving the equations of motion for porous isotropic media," *J. Acoust. Soc. Am.*, vol. 92, pp. 3278–3290, Dec. 1992.

[41] S. R. Pride, F. D. Morgan, and A. F. Gangi, "Drag forces of porous-medium acoustics," *Phys. Rev. B*, vol. 47, pp. 4964–4978, Mar. 1993.

[42] D. Lafarge, "Comments on "Rigorous link between fluid permeability, electric conductivity, and relaxation times for transport in porous media"," *Phys. Fluids A-Fluid*, vol. 5, pp. 500–502, Feb. 1993.

[43] D. Lafarge, P. Lemarinier, J.-F. Allard, and V. Tarnow, "Dynamic compressibility of air in porous structures at audible frequencies," *J. Acoust. Soc. Am.*, vol. 102, pp. 1995–2006, Oct. 1997.

[44] S. Gasser, F. Paun, and Y. Bréchet, "Absorptive properties of rigid porous media: Application to face centered cubic sphere packing," *J. Acoust. Soc. Am.*, vol. 117, pp. 2090–2099, Apr. 2005.

[45] C.-Y. Lee, M. J. Leamy, and J. H. Nadler, "Acoustic absorption calculation in irreducible porous media: A unified computational approach," *J. Acoust. Soc. Am.*, vol. 126, pp. 1862–1870, Oct. 2009.

[46] C. Perrot, F. Chevillotte, and R. Panneton, "Bottom-up approach for microstructure optimization of sound absorbing materials," *J. Acoust. Soc. Am.*, vol. 124, pp. 940–948, Aug. 2008.

[47] T. G. Zieliński, "Microstructure-based calculations and experimental results for sound absorbing porous layers of randomly packed rigid spherical beads," *J. Appl. Phys.*, vol. 116, pp. 1–17, article 034905, July 2014.

[48] M. S. Alnæs, J. Blechta, J. Hake, A. Johansson, B. Kehlet, A. Logg, C. Richardson, J. Ring, M. E. Rognes, and G. N. Wells, "The FEniCS Project version 1.5," *Arch. Num. Soft.*, vol. 3, pp. 9–23, Dec. 2015.

[49] O. C. Zienkiewicz, R. L. Taylor, and J. Z. Zhu, *The finite element method: Its basis and fundamentals*. Butterworth-Heinemann, 7 ed., Aug. 2013.